

Impact of Moderate Blast Exposures on Thrombin Biomarkers Assessed by Calibrated Automated Thrombography in Rats

Victor Prima,^{1,2} Victor L. Serebruany,³ Artem Svetlov,¹ Ronald L. Hayes,¹ and Stanislav I. Svetlov^{1,2}

Abstract

Severe blast exposures are frequently complicated with fatal intracranial hemorrhages. However, many more sustain low level blasts without tissue damage detectable by brain imaging. To investigate effects of nonlethal blast on thrombin-related biomarkers, rats were subjected to two different types of head-directed blast: 1) moderate “composite” blast with strong head acceleration or 2) moderate primary blast, without head acceleration. Thrombin generation (TG) *ex vivo* after blast was studied by calibrated automated thrombography (CAT). In the same blood samples, we assessed maximal concentration of TG (TG_{max}), start time, peak time, mean time, and concentrations of protein markers for vascular/hemostatic dysfunctions: integrin α/β , soluble endothelial selectin (sE-selectin), soluble intercellular cell adhesion molecule-1 (sICAM-1), and matrix metalloproteinases (MMP)-2, MMP-8, and MMP-13. Blast remarkably affected all TG indices. In animals exposed to “composite” blast, TG_{max} peaked at 6 h (~4.5-fold vs. control), sustained at day 1 (~3.8-fold increase), and declined to a 2-fold increase over control at day 7 post-blast. After primary blast, TG_{max} also rose to ~4.2-fold of control at 6 h, dropped to ~1.7-fold of control at day 1, and then exhibited a slight secondary increase at 2-fold of control at day 7. Other TG indices did not differ significantly between two types of blast exposure. The changes were also observed in other microvascular/inflammatory/hemostatic biomarkers. Integrin α/β and sICAM-1 levels were elevated after both “composite” and primary blast at 6 h, 1 day, and 7 days. sE-selectin exhibited near normal levels after “composite” blast, but increased significantly at 7 days after primary blast; MMP-2, MMP-8, and MMP-13 slightly rose after “composite” blast and significantly increased (~2–4-fold) after primary blast. In summary, CAT may have a clinical diagnostic utility in combination with selected set of microvascular/inflammatory biomarkers in patients subjected to low/moderate level blast exposures.

Key words: animal studies; biomarkers; cerebral vascular disease; traumatic brain injury

Introduction

BLAST-RELATED TRAUMATIC BRAIN INJURY (TBI) is the most common combat-related injury that “has emerged as a leading injury among service members” on the battlefield,¹ while the proportion of civilian casualties caused by explosives has increased as well.² TBI can lead to sustained neuro-somatic damage and neuro-degeneration,³ especially when repeated. As the over-pressurization wave propagates through the body, a blast generates primary damage at gas–fluid interfaces,⁴ including pulmonary barotraumas, tympanic membrane ruptures with middle ear damage, abdominal hemorrhage and perforation, rupture of the eyeballs, and concussions.⁵ Pulmonary barotraumas, together with TBI, are the most common fatal primary blast injuries, including free radical-associated injuries such as thrombosis, lipoyxygenation, and dis-

seminated intravascular coagulation. TBI-related coagulopathies substantially increase the risk of death and disability both in civilian⁶ and military⁷ settings. Current research suggests that blast injury and/or hemorrhage leads to hypotensive and hypoxemic secondary injury and impairs cerebral vascular compensatory responses.⁸ Therefore, the effects of mild blast injury on the critical components of hemostasis are of high importance for the development of novel TBI diagnostics and therapeutics, and warrant more in-depth investigation.

Thrombin, or activated factor II, is a protease in the bloodstream that plays a key role in the modulation of hemostasis in general, but specifically in the activation of the coagulation cascade. Thrombin is produced by enzymatic cleavage of prothrombin by activated factor X, and is required to convert soluble protein fibrinogen into insoluble fibrin, promoting formation of a clot.^{9,10} In addition,

¹Banyan Laboratories, Inc., Alachua, Florida.

²Departments of Medicine and Urology, University of Florida, Gainesville, Florida.

³Heart Drug Research LLC, Towson, Maryland.

thrombin is believed to affect other biological activities in various cell types, including endothelial cells¹¹ and platelets.¹² Being a potent vasoconstrictor and mitogen, thrombin is recognized as a contributor to both acute and prolonged vasospasm, playing an important role in the pathogenesis of stroke by promoting cerebral ischemia, and/or enhancing risks for intracranial hemorrhage.¹³ Several studies identified thrombin as an important contributor to the pathological developments following various injury types.^{14,15}

Therefore, assessing thrombin activity represents an attractive, and potentially clinically useful, diagnostic tool for blast-related injury triage.

However, considering fast cleavage and aggressive binding patterns, measurement of thrombin activity is challenging. The most reliable among presently available tests is serial assessment of thrombin in plasma as a function of time, by comparing the fluorescent signal from a thrombin-generating sample using the calibrated automated thrombography (CAT) method, developed by Hemker and colleagues.^{16,17} Applying the CAT system, we determined the blast wave-induced effects on multiple indices of thrombin generation (TG) potential and compared them with concomitant changes of several other markers of coagulation/inflammation vessel wall crosstalk. Using these proteins as a supplementary biomarkers panel for TBI diagnostics can validate and support otherwise injury type-nonspecific CAT data.

Methods

Blast generator design and setup

The compressed air-driven shock tube, capable of generating a wide range of controlled blast waves, has been described in detail previously.¹⁸ The tube consists of two sections: high-pressure (driver) and low-pressure (driven) separated by a diaphragm. Peak overpressure (OP), composition, and duration of the generated high pressure shockwaves are determined by the shock tube configuration, including thickness, type of diaphragm material, driver/driven length ratio, and the initial driver pressure at the moment of diaphragm rupture. In the presented series of experiments, we employed different spatial setups as will be described subsequently. The blast pressure data were acquired using PCB Piezoelectric blast pressure transducers and LabView 8.2 software. A National Instruments 1.25 M samples/sec data acquisition card was used to acquire data from multiple channels. The rat head images during the blast event were captured at 40,000 frames/sec using a high speed video camera (Phantom V310, Vision Research, Wayne, NJ).

Animal exposure to a controlled blast wave

Modeling of the primary blast and the “composite” OP load was achieved by variable positioning of the target versus the blast generator. All rats were anesthetized with isoflurane inhalations, described previously in detail. After reaching a deep plane of anesthesia, they were placed into a holder exposing only their heads (body-armored setup) at a distance 5 cm below the exit nozzle of the shock tube. Rats were positioned either directly on the shock tube axis ($n=5$) to expose them to the “composite” blast including the compressed air jet (Fig. 1 A, B) or at the 45 degree angle to it ($n=6$) for exposure only to the primary blast wave (Fig. 1 D, E). Animals were then subjected to a single blast with a mean peak OP of 230–380 kPa at the target. The exact static and dynamic overpressure values depending upon the angle and distance of rat head from the nozzle of shock tube were established during the prior calibration tests. The control group of animals ($n=4$) underwent the same treatment (anesthesia, handling, recovery), except they were not exposed to a blast.

Blood collection

At the required time points following blast exposure, animals were euthanized according to guidelines approved by the Institutional Animal Care and Use Committee (IACUC) of the University of Florida. With the animal under isoflurane anesthesia, blood was withdrawn directly from the heart with an 18 gauge needle, and processed to obtain plasma and serum. One half of collected blood aliquot was drawn into 0.5 mL Capiject EDTA (K2) tubes (Terumo, Elkton, MD) at room temperature. The Capiject tube was gently inverted three to five times to ensure complete mixing of the anticoagulant. Platelet poor plasma (PPP) was centrifuged at 6000g for 15 min at room temperature, and frozen at -80°C until analysis. Another half of the blood aliquot was drawn into Multivette 600 tubes with clotting activator (Sarstedt, Nümbrecht, Germany) and was allowed to clot at room temperature for 40 min. Serum was separated by centrifugation at 10,000g for 5 min and frozen at -80°C until analysis. All samples were labeled with a coded number and analyzed by blinded technicians.

Antibody-based assays

Custom Biotin Label-based (L-series) RatAntibody arrays (Ray Biotech, Norcross, GA) were used to assess relative levels of integrin α/β , soluble endothelial selectin (sE-selectin), and matrix metalloproteinases (MMP)-2, MMP-8 and MMP-13 in rat serum following blast exposure. Commercially available Sandwich ELISA kits for soluble intercellular adhesion molecule-1 (soluble intercellular cell adhesion molecule-1 [sICAM-1]; CUSABIO Biotech) were used according to the manufacturer’s instructions.

CAT reagents

Fluobuffer containing 20 mM HEPES and 60 mg/mL bovine serum albumin (Sigma, St. Louis, MO) were prepared *ex tempore* on the day of the experiment. Working buffer consisted of 140 mM NaCl, 20 mM HEPES, and 5 mg/mL human serum albumin. The fluorogenic substrate Z-Gly-Gly-Arg-amino-methyl-coumarin (Bachem, Bubendorf, Switzerland) was solubilized in pure dimethylsulfoxide (DMSO, Sigma, St. Louis, MO). The PPP reagent with a content of 5 pM tissue factor, and the thrombin calibrator (Thrombinoscope BV, Maastricht, Netherlands), was provided by Diagnostica Stago (Parsippany, NJ).

CAT

Measurement of TG potential was performed using the CAT system. The validation details of the method are described elsewhere.^{16,17,19} Briefly, for each experiment, a fresh mixture of fluobuffer and CaCl₂ solution was prepared and incubated for 5 min at 37°C. After 5 min, 75 μL of the Fluo-DMSO-solution were added, mixed and incubated for a further 5 min. The resulting clear solution was referred to as FluCa. PPP reagent was solubilized with 2 mL deionized water. Twenty microliters of this trigger solution were put into each sample well of a 96 well round-bottom microtiter plate made of polypropylene (Nunc, Roskilde, Denmark). After reconstitution with 1 mL sterile water, the thrombin calibrator was used in each experiment to compare the simultaneously measured thrombin activity in the sample with that from a known and stable concentration in the calibrator well. Finally, 80 μL of plasma were put into each well. The 96 well plate was then placed in the fluorometer (Fluoroskan Ascent, Thermolabsystems OY, Helsinki, Finland) with an excitation filter at 390 nm and an emission filter at 460 nm. The automated dispensing of 20 μL FluCa indicated the onset of measurement of thrombin indices. Each well was measured every 20 sec for the duration of 40 min. Each experiment was performed fourfold. We used Analysis Software from Diagnostica Stago, Inc. (Parsippany, NJ) to assess four indices, namely TG_{max}

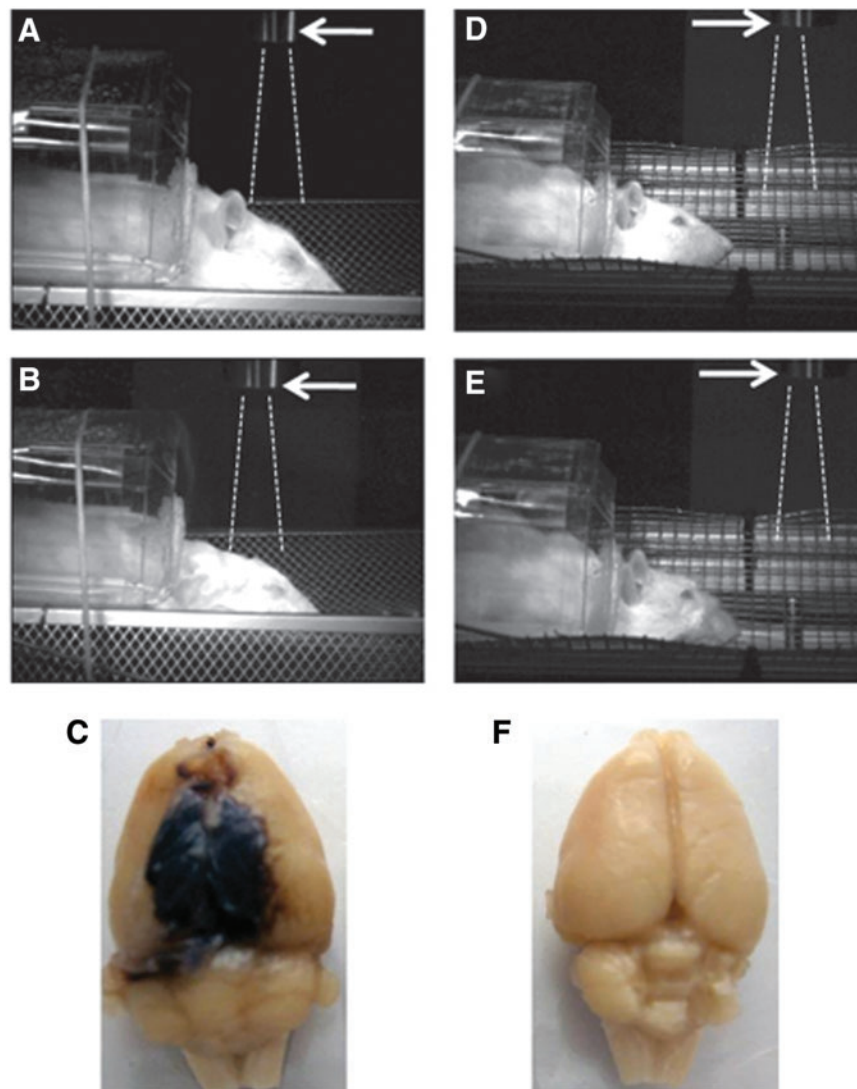


FIG. 1. Rat models of brain injury with “composite” or primary blast overpressure. High speed video images recorded before (**A, D**) and after (**B, E**) blast wave passage illustrate rat head movement on “composite” on-axis (**A, B**) versus primary off-axis (**D, E**) blast wave load for 10 msec. Arrows indicate the shock tube exit. Dashed lines depict trajectory of compressed air jet. Brain pathomorphology after head-directed exposure to blast wave: anesthetized rats were subjected to a “composite” (**C**) or a primary (**F**) blast overpressure load as described in the Methods section. Forty-eight hours after exposures brains were perfused *in situ*, removed, and recorded. Gross pathology: typical focal intracranial hematomas observed following “composite” overpressure load of 230–380 kPa. Color images are available online at www.liebertpub.com/neu

(max concentration of TG), start time (t-start) peak time (t-peak), and mean time (t-mean).

Statistical analysis

The Mann–Whitney *U* test was used to analyze nonparametric data. Normally distributed data were expressed as mean \pm SD, and skewed data as median (range). All *p* values were two sided, with the significance level set at 0.05. Statistical analyses were performed using GraphPad Prism (GraphPad Software, La Jolla, CA).

Results

Blast-induced gross pathology

The high speed video recordings shown in Figure 1 present different biomechanics of target movement on the load of the “composite” or primary blast. Significant head acceleration and

deformation after “composite” blast exposure (Fig. 1 A, B) were accompanied by typical focal and massive intracranial hematomas and brain swelling. The hemorrhages and hematomas developed within hours after impact and appeared visibly through the undamaged skull at 24–48 h after blast exposure (data not shown). The size of hematomas varied significantly in different rats and formed a capsule at 5 days post-blast, as shown in one of the most damaged rat brains after *in situ* perfusion (Fig. 1 C). The intracranial blood accumulation partially resolved at day 14 in a majority of rats observed (data not shown). On the other hand, primary blast exposure in the described model did not lead to noticeable hematomas.

Thrombin biomarkers

The combined data on TG potential at different time points and blast setups are presented in the Table 1.

TABLE 1. INDICES OF THROMBIN ACTIVITY AFTER EXPOSURE TO A PRIMARY/COMPOSITE BLAST WAVE LOAD

	CAT parameter	Baseline	6 h post-blast	1 day post-blast	7 days post-blast
Primary blast	TG _{max} (nM)	121.0 ± 38.0	513.0 ± 44.0*	212.0 ± 68.0*	255.0 ± 49.0*
	t (peak) (min)	4.8 ± 0.19	8.0 ± 0.24*	7.0 ± 0.12*	5.0 ± 0.11*
	t (start) (min)	1.1 ± 0.07	1.0 ± 0.08*	1.0 ± 0.09*	1.0 ± 0.07*
	t (mean) (min)	6.4 ± 0.17	5.4 ± 0.18*	4.5 ± 0.15*	4.0 ± 0.13*
	CAT parameter	Baseline	6 h post-blast	1 day post-blast	7 days post-blast
Composite blast	TG _{max} (nM)	120.1 ± 7.2	540.0 ± 26.1*	450.0 ± 23.3*	250.0 ± 11.1*
	t (peak) (min)	5.0 ± 0.14	8.0 ± 0.13*	7.0 ± 0.13*	5.0 ± 0.10
	t (start) (min)	1.2 ± 0.08	1.0 ± 0.07*	1.0 ± 0.06*	1.0 ± 0.06*
	t (mean) (min)	6.4 ± 0.12	5.5 ± 0.13*	4.5 ± 0.11*	4.0 ± 0.10*

**p* value < 0.05 versus naïve samples.

CAT, calibrated automated thrombography.

All indices of TG were remarkably affected in all blast-exposed rats compared with naïve animals. However, in “composite” blast-exposed animals, TG_{max} peaked at 6 h (~4.5-fold vs. control), sustained at 1 day (~3.8-fold increase), and declined to a 2-fold increase over control levels at day 7 post-blast. In rats subjected to primary blast, TG_{max} also rose to ~4.2-fold of control values at 6 h, dropped to ~1.7-fold of control levels at 1 day post-blast, and then exhibited a secondary increase to 2-fold of control values at day 7 post-blast (Fig. 2A).

Other TG indices did not differ significantly between two types of blast exposure. After either “composite” or primary blast loads, the t-peak times significantly increased compared with control values, whereas corresponding t-mean values decreased at both blast setups. The representative overlapped TG tracings after a primary blast wave load are illustrated in Figure 2B.

The cumulative analysis of the data suggests strong time-dependent stimulation of overall TG potential by blast exposure.

Blast-induced expression induction of hemostasis-related proteins

Integrin α/β levels in serum were raised at both blast setups, indicating that overpressure wave load is triggering microcirculatory disorders whether it produces head hyperacceleration or not (Fig. 3A). After blast, the integrin α/β levels stayed elevated at both assayed time points: 1 day and 7 days. Soluble E-selectin displayed stable serum levels after “composite” blast, but increased significantly at 7 days after primary blast (Fig. 3B). Soluble ICAM-1 levels were elevated in serum at both blast setups from 6 h to 7 days post-blast, most significantly (approximately fourfold of control) at 6 h after “composite” and 7 days after primary blast (Fig. 3C). MMP-2, MMP-8, and MMP-13 displayed similar post-blast responses: slight elevation of relative serum concentrations after “composite” blast and significant increase (~2–4-fold) after primary blast (Fig. 3D–F).

Discussion

Our previous studies^{18,20} suggested that blast wave composition should be taken into account in the explosive blast modeling with compressed gas-driven shock tubes. Here we explored the impact on hemostasis of two different types of blast: 1) moderate composite (head on-axis) blast with strong head acceleration, and 2) moderate primary off-axis blast load on the frontal part of rat skull without head acceleration. There have been multiple studies^{20–23}

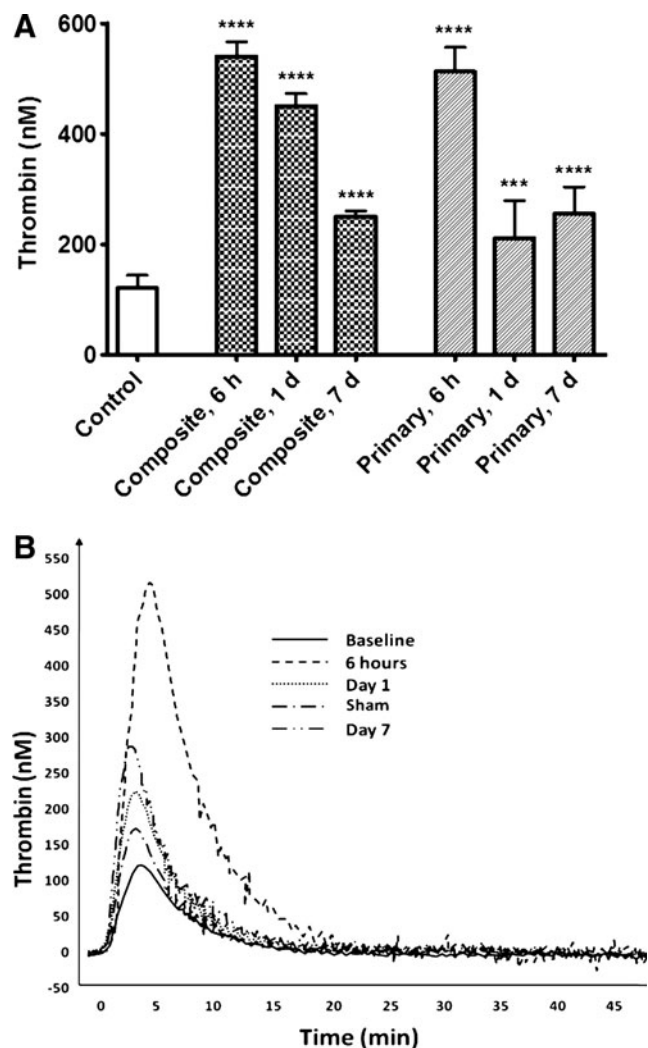


FIG. 2. Plasma levels of thrombin after blast. Thrombin generation potential was assessed in rat plasma by calibrated automated thrombography (CAT) technology (A). Representative thrombography tracings after primary blast exposure (B). Please see Methods section for details. Blood was collected from overpressure (OP)-exposed rats at different time-points and shock tube set-ups. Data shown are mean ± SEM of four independent experiments. ****p* < 0.001; *****p* < 0.0001 versus control samples.

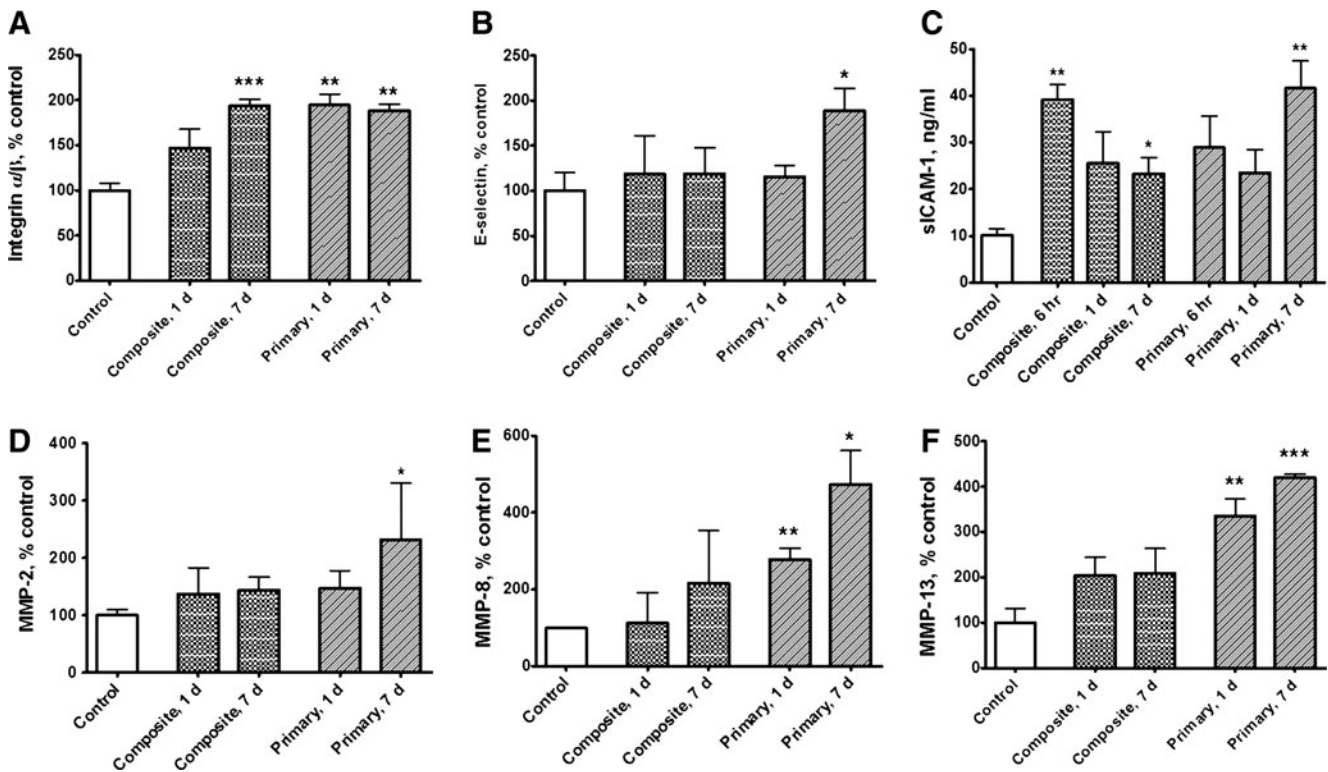


FIG. 3. Serum levels of hemostasis-related proteins after blast. Concentrations of integrin α/β (A), soluble endothelial selectin (E-selectin) (B), soluble intercellular cell adhesion molecule-1 (ICAM-1) (C) and matrix metalloproteinases (MMP)-2 (D), MMP-8 (E), and MMP-13 (F) were assessed in rat serum by antibody arrays and ELISA. Please see Methods section for details. Blood was collected from overpressure (OP)-exposed rats at different shock tube setups. Data shown are mean \pm SEM of four to six independent experiments. * $p < 0.05$; ** $p < 0.005$; *** $p < 0.001$ vs. control samples.

showing that angular and linear head accelerations (“bobblehead effect”) have much more severe impact than primary blast wave passing through the brain tissue. Moreover, some studies suggest that angular accelerations generate more powerful pressures in the brain than do linear accelerations.^{24,25} Also, because of the presence of compressed air jet in the “composite” blast wave, the target experienced much higher OP impact resulting in intracranial hematomas (the typical post-blast gross pathology represented in Fig. 1 C).

In mammals, hemostasis is achieved through primary platelet activation-aggregation and secondary coagulation cascade. TBI induces loss of equilibrium in tightly regulated hemostatic systems, which can lead to either hypercoagulable states with microthrombosis and ischemia, or hypocoagulable states with possible progression of hemorrhagic lesions.²⁶ In our studies, only the animal’s head was exposed to blast waves, because of a rigid protective shield covering the rest of the body. Nevertheless, hemostasis-related indices were strongly affected in the peripheral blood. TG, the key process in the secondary hemostasis, was strongly affected by blast exposure. Usually thrombin levels are difficult to measure, and TG is commonly assessed indirectly through either enzyme-inhibitor complexes or prothrombin cleavage fragments. In our studies, we employed a novel method, CAT, which has been used recently for analysis of hemostasis in stroke patients.²⁷ As the data presented in Table 1 and further illustrated by Figure 2 show, all indices of TG were remarkably affected in all blast-exposed rats compared with control animals. An early more than fivefold spike of TG gradually decreased over 7 days post-

blast, but still significantly exceeded the control values, suggesting it as a potential candidate for a clinical biomarker.

Following the blast, we observed coincident changes in the other important coagulation and inflammation factors in the hemostasis cascade, which exhibited trends in agreement with TG upregulation. However, contrary to the initial expectations, serum levels of the biomarkers studied after “composite” blast with strong head acceleration did not in general exceed corresponding levels after primary blast. In this respect, coagulation/inflammation biomarker data oppose our blast-induced gross pathology findings (Fig. 1A–C), and the existing hypothesis that head acceleration-deceleration resulting from blast forces exerted on the skull (“bobblehead effect”) would be the prevailing cause of persistent brain injury.²³ As shown in Figure 3, serum integrin α/β concentrations were raised after either primary or composite blast exposures and remained significantly elevated up to 7 days post-blast. It is known that the integrins, a large family of cell surface receptors, play pivotal roles in platelet adhesion and aggregation, white cell/endothelium interactions, and platelet-mediated thrombin generation.²⁸ Our findings are in line with the available data, which indicate that vascular injury is a stimulus for expression of α/β integrins by vascular cells.²⁹ Concomitant rise of thrombin and integrin α/β reflects important interplay between thrombin and $\beta 3$ -integrins in hemostasis. Thrombin, by binding to G protein coupled, protease-activated receptors, is a potent activator of integrins. Conversely, outside-in signaling through integrins amplifies events initiated by thrombin, and is necessary for full platelet spreading, platelet aggregation, and the formation of a stable platelet thrombus.³⁰

As was shown in animal models of TBI, an influx of peripheral blood cells through disrupted blood-brain barrier (BBB) begins within hours after injury.³¹ Multiple TBI-related animal studies^{32,33} and clinical data^{34,35} in agreement with our findings (Fig. 3 B, C) also demonstrate significant elevation in serum of inflammatory cell adhesion molecules, such as sICAM-1 and sE-selectin, which bind to circulating leukocytes and facilitate their migration into the injured brain regions. Endothelial pro-inflammatory processes are potently induced by thrombin.^{36–38} Adverse effects of inflammatory response to injury are reflected by highly significant relationship between serum sICAM-1 and poor neurological outcome.^{35,39}

Another group of molecules deeply involved in the neuroinflammation processes, MMPs, are known to be rapidly upregulated in patients with TBI,⁴⁰ and contribute to BBB breakdown⁴¹ by degrading tight-junction proteins.⁴² The consequent increase in blood vessel permeability^{43,44} facilitates the development of edema. Our observations that MMP-2, MMP-8, and MMP-13 increase following primary blast wave exposure (Fig. 3 D–F) support the current vision of the diverse mechanisms of MMPs' involvement in brain injury either directly through degradation of brain matrix-substrates or indirectly through interaction with other bioactive molecules,⁴⁵ including thrombin^{46,47} and integrin.⁴⁸ At this point, we do not have sufficient explanation as to why MMPs' levels after primary blast significantly exceed their levels after “composite” blast with strong head acceleration. If confirmed by independent studies, this effect may have a special advantage for the detection of mild blast-induced vascular abnormalities in the absence of the “boblehead effect” accompanied by severe hematomas.

Only recently has the development of compressed gas-driven blast wave generators with controlled OP enabled quantitative assessment of closed head blast TBI *in vivo*.^{18,23,49,50} Analysis of the details of blast wave interaction with the target in the animal models have set it apart both from the civilian accidental TBI cases and from the penetrating brain injuries.²⁰ Notably, blast-induced closed head injuries are rarely as gruesome as their open counterparts, even though they can be just as damaging. Because these injuries neither puncture the dura mater nor necessarily breach the skull or scalp, they tend to be very hard to detect in the field or even in the hospital, as conventional imaging techniques such as MRI, functional MRI (fMRI), and CT can only detect gross internal deformities. Especially difficult is the objective assessment of mild blast trauma severity when the apparent trauma signs are benign or hidden.^{1,3} As discussed previously,^{51,52} vasospasm and rapidly developing diffuse cerebral edema leading to intracranial hypertension have been identified among the unique hallmarks of blast-induced closed head injuries encountered in military and civilian settings, which underlines the need for adequate diagnostic tools for hemodynamic and hemostatic abnormalities. Because thrombin, a central molecule in coagulation, is also involved in inflammation,⁵³ it positions TG among potential biomarkers for predicting neurological outcome after blast-induced TBI. Further human studies would be required to evaluate its clinical applications. Assessing TG potential, in combination with a carefully selected panel of blood biomarkers related to the cerebral hemostasis disruption, may be an attractive and reliable diagnostic tool for mild blast-related injury triage.

Acknowledgments

The authors thank Danny Johnson for his expert technical assistance. This work was supported by grants W81XWH-8-1-0376 and W81XWH-07-01-0701 from the Department of Defense.

Author Disclosure Statement

No competing financial interests exist.

References

- Kanof, M. (2008). VA HEALTH CARE: Mild Traumatic Brain Injury Screening and Evaluation Implemented for OEF/OIF Veterans, but Challenges Remain. Washington DC: U.S. Government Printing Office.
- Coupland, R.M., and Samnegaard, H.O. (1999). Effect of type and transfer of conventional weapons on civilian injuries: retrospective analysis of prospective data from Red Cross hospitals. *BMJ* 319, 410–412.
- Chen, Y., and Huang, W. (2011). Non-impact, blast-induced mild TBI and PTSD: concepts and caveats. *Brain Inj.* 25, 641–650.
- Guy, R.J., Glover, M.A., and Cripps, N.P. (1998). The pathophysiology of primary blast injury and its implications for treatment. Part I: The thorax. *J. R. Nav. Med. Serv.* 84, 79–86.
- Wightman, J.M., and Gladish, S.L. (2001). Explosions and blast injuries. *Ann. Emerg. Med.* 37, 664–678.
- Harhangi, B.S., Kompanje, E.J., Leebeek, F.W., and Maas, A.I. (2008). Coagulation disorders after traumatic brain injury. *Acta Neurochir. (Wien)* 150, 165–175.
- Cap, A.P., and Spinella, P.C. (2011). Severity of head injury is associated with increased risk of coagulopathy in combat casualties. *J. Trauma* 71, S78–81.
- DeWitt, D.S., and Prough, D.S. (2009). Blast-induced brain injury and posttraumatic hypotension and hypoxemia. *J. Neurotrauma* 26, 877–887.
- Bode, W. (2006). Structure and interaction modes of thrombin. *Blood Cells Mol. Dis.* 36, 122–130.
- Wolberg, A.S. (2007). Thrombin generation and fibrin clot structure. *Blood Rev.* 21, 131–142.
- Lockard, M.M., Witkowski, S., Jenkins, N.T., Spangenburg, E.E., Obisesan, T.O., and Hagberg, J.M. (2010). Thrombin and exercise similarly influence expression of cell cycle genes in cultured putative endothelial progenitor cells. *J. Appl. Physiol.* 108, 1682–1690.
- Sosdorf, M., Konig, V., Gummert, J., Marx, G., and Losche, W. (2008). Correlations between platelet-derived microvesicles and thrombin generation in patients with coronary artery disease. *Platelets* 19, 476–477.
- Kang, D.W., Yoo, S.H., Chun, S., Kwon, K.Y., Kwon, S.U., Koh, J.Y., and Kim, J.S. (2009). Inflammatory and hemostatic biomarkers associated with early recurrent ischemic lesions in acute ischemic stroke. *Stroke* 40, 1653–1658.
- Groves, H.M., Kinlough–Rathbone, R.L., Richardson, M., Jorgensen, L., Moore, S., and Mustard, J.F. (1982). Thrombin generation and fibrin formation following injury to rabbit neointima. Studies of vessel wall reactivity and platelet survival. *Lab. Invest.* 46, 605–612.
- Walters, T.K., Gorog, D.A., and Wood, R.F. (1994). Thrombin generation following arterial injury is a critical initiating event in the pathogenesis of the proliferative stages of the atherosclerotic process. *J. Vasc. Res.* 31, 173–177.
- Hemker, H.C., Giesen, P., Al Dieri, R., Regnault, V., de Smedt, E., Wagenvoort, R., Lecompte, T., and Beguin, S. (2003). Calibrated automated thrombin generation measurement in clotting plasma. *Pathophysiol. Haemost. Thromb.* 33, 4–15.
- Hemker, H.C., Giesen, P., AlDieri, R., Regnault, V., de Smed, E., Wagenvoort, R., Lecompte, T., and Beguin, S. (2002). The calibrated automated thrombogram (CAT): a universal routine test for hyper- and hypocoagulability. *Pathophysiol. Haemost. Thromb.* 32, 249–253.
- Svetlov, S.I., Prima, V., Kirk, D.R., Gutierrez, H., Curley, K.C., Hayes, R.L., and Wang, K.K. (2010). Morphologic and biochemical characterization of brain injury in a model of controlled blast overpressure exposure. *J. Trauma* 69, 795–804.
- Luddington, R., and Baglin, T. (2004). Clinical measurement of thrombin generation by calibrated automated thrombography requires contact factor inhibition. *J. Thromb. Haemost.* 2, 1954–1959.
- Svetlov, S.I., Prima, V., Glushakova, O., Svetlov, A., Kirk, D.R., Gutierrez, H., Serebruany, V.L., Curley, K.C., Wang, K.K., and Hayes, R.L. (2012). Neuro-glial and systemic mechanisms of pathological responses in rat models of primary blast overpressure compared to “composite” blast. *Front. Neurol.* 3, 15.
- Risling, M., Plantman, S., Angeria, M., Rostami, E., Bellander, B.M., Kirkegaard, M., Arborelius, U., and Davidsson, J. (2011). Mechanisms

- of blast induced brain injuries, experimental studies in rats. *Neuroimage* 54, Suppl. 1, S89–97.
22. Fijalkowski, R.J., Stemper, B.D., Pintar, F.A., Yoganandan, N., Crowe, M.J., and Gennarelli, T.A. (2007). New rat model for diffuse brain injury using coronal plane angular acceleration. *J Neurotrauma* 24, 1387–1398.
 23. Goldstein, L.E., Fisher, A.M., Tagge, C.A., Zhang, X.L., Velisek, L., Sullivan, J.A., Upreti, C., Kracht, J.M., Ericsson, M., Wojnarowicz, M.W., Goletiani, C.J., Maglakelidze, G.M., Casey, N., Moncaster, J.A., Minaeva, O., Moir, R.D., Nowinski, C.J., Stern, R.A., Cantu, R.C., Geiling, J., Blusztajn, J.K., Wolozin, B.L., Ikezu, T., Stein, T.D., Budson, A.E., Kowall, N.W., Chargin, D., Sharon, A., Saman, S., Hall, G.F., Moss, W.C., Cleveland, R.O., Tanzi, R.E., Stanton, P.K., and McKee, A.C. (2012). Chronic traumatic encephalopathy in blast-exposed military veterans and a blast neurotrauma mouse model. *Sci. Transl. Med.* 4, 134–160.
 24. Zhang, J., Yoganandan, N., Pintar, F.A., and Gennarelli, T.A. (2006). Role of translational and rotational accelerations on brain strain in lateral head impact. *Biomed Sci Instrum* 42, 501–506.
 25. Krave, U., Hojer, S., and Hansson, H.A. (2005). Transient, powerful pressures are generated in the brain by a rotational acceleration impulse to the head. *Eur J Neurosci* 21, 2876–2882.
 26. Laroche, M., Kutcher, M.E., Huang, M.C., Cohen, M.J., and Manley, G.T. (2012). Coagulopathy following traumatic brain injury. *Neurosurgery* 70, 1334–1345.
 27. Serebruany, V., Sani, Y., Lynch, D., Schevchuck, A., Svetlov, S., Fong, A., Thevathasan, L., and Hanley, D. (2012). Effects of dabigatran in vitro on thrombin biomarkers by calibrated automated thrombography in patients after ischemic stroke. *J. Thromb. Thrombolysis* 33, 22–27.
 28. Ni, H., and Freedman, J. (2003). Platelets in hemostasis and thrombosis: role of integrins and their ligands. *Transfus. Apher. Sci.* 28, 257–264.
 29. Stouffer, G.A., Hu, Z., Sajid, M., Li, H., Jin, G., Nakada, M.T., Hanson, S.R., and Runge, M.S. (1998). Beta3 integrins are upregulated after vascular injury and modulate thrombospondin- and thrombin-induced proliferation of cultured smooth muscle cells. *Circulation* 97, 907–915.
 30. Stouffer, G.A., and Smyth, S.S. (2003). Effects of thrombin on interactions between beta3-integrins and extracellular matrix in platelets and vascular cells. *Arterioscler. Thromb. Vasc. Biol.* 23, 1971–1978.
 31. Ghajar, J. (2000). Traumatic brain injury. *Lancet* 356, 923–929.
 32. Chen, G., Shi, J., Hu, Z., and Hang, C. (2008). Inhibitory effect on cerebral inflammatory response following traumatic brain injury in rats: a potential neuroprotective mechanism of N-acetylcysteine. *Mediators Inflamm* 2008, 716458.
 33. Balabanov, R., Goldman, H., Murphy, S., Pellizon, G., Owen, C., Rafols, J., and Dore-Duffy, P. (2001). Endothelial cell activation following moderate traumatic brain injury. *Neurol. Res.* 23, 175–182.
 34. Yilmaz, G., and Granger, D.N. (2008). Cell adhesion molecules and ischemic stroke. *Neurol. Res.* 30, 783–793.
 35. Wang, H.C., Lin, W.C., Lin, Y.J., Rau, C.S., Lee, T.H., Chang, W.N., Tsai, N.W., Cheng, B.C., Kung, C.T., and Lu, C.H. (2011). The association between serum adhesion molecules and outcome in acute spontaneous intracerebral hemorrhage. *Crit. Care* 15, R284.
 36. Miho, N., Ishida, T., Kuwaba, N., Ishida, M., Shimote-Abe, K., Tabuchi, K., Oshima, T., Yoshizumi, M., and Chayama, K. (2005). Role of the JNK pathway in thrombin-induced ICAM-1 expression in endothelial cells. *Cardiovasc. Res.* 68, 289–298.
 37. Kaplanski, G., Marin, V., Fabrigoule, M., Boulay, V., Benoliel, A.M., Bongrand, P., Kaplanski, S., & Farnarier, C. (1998). Thrombin-activated human endothelial cells support monocyte adhesion in vitro following expression of intercellular adhesion molecule-1 (ICAM-1; CD54) and vascular cell adhesion molecule-1 (VCAM-1; CD106). *Blood* 92, 1259–1267.
 38. Alabanza, L.M., and Bynoe, M.S. (2012). Thrombin induces an inflammatory phenotype in a human brain endothelial cell line. *J. Neuroimmunol.* 245, 48–55.
 39. McKeating, E.G., Andrews, P.J., and Mascia, L. (1998). The relationship of soluble adhesion molecule concentrations in systemic and jugular venous serum to injury severity and outcome after traumatic brain injury. *Anesth. Analg.* 86, 759–765.
 40. Vilalta, A., Sahuquillo, J., Rosell, A., Poca, M.A., Riveiro, M., and Montaner, J. (2008). Moderate and severe traumatic brain injury induce early overexpression of systemic and brain gelatinases. *Intensive Care Med.* 34, 1384–1392.
 41. Petty, M.A., and Lo, E.H. (2002). Junctional complexes of the blood–brain barrier: permeability changes in neuroinflammation. *Prog. Neurobiol.* 68, 311–323.
 42. Yang, Y., Estrada, E.Y., Thompson, J.F., Liu, W., and Rosenberg, G.A. (2007). Matrix metalloproteinase-mediated disruption of tight junction proteins in cerebral vessels is reversed by synthetic matrix metalloproteinase inhibitor in focal ischemia in rat. *J. Cereb. Blood Flow Metab.* 27, 697–709.
 43. Harkness, K.A., Adamson, P., Sussman, J.D., Davies–Jones, G.A., Greenwood, J., and Woodroffe, M.N. (2000). Dexamethasone regulation of matrix metalloproteinase expression in CNS vascular endothelium. *Brain* 123, 698–709.
 44. Suehiro, E., Fujisawa, H., Akimura, T., Ishihara, H., Kajiwara, K., Kato, S., Fujii, M., Yamashita, S., Maekawa, T., and Suzuki, M. (2004). Increased matrix metalloproteinase-9 in blood in association with activation of interleukin-6 after traumatic brain injury: influence of hypothermic therapy. *J Neurotrauma* 21, 1706–1711.
 45. Moranco, A., Rosell, A., Garcia–Bonilla, L., and Montaner, J. (2010). Metalloproteinase and stroke infarct size: role for anti-inflammatory treatment? *Ann. N. Y. Acad. Sci.* 1207, 123–133.
 46. Orbe, J., Rodriguez, J.A., Calvayrac, O., Rodriguez–Calvo, R., Rodriguez, C., Roncal, C., Martinez de Lizarrondo, S., Barrenetxe, J., Riverter, J.C., Martinez–Gonzalez, J., and Paramo, J.A. (2009). Matrix metalloproteinase-10 is upregulated by thrombin in endothelial cells and increased in patients with enhanced thrombin generation. *Arterioscler. Thromb. Vasc. Biol.* 29, 2109–2116.
 47. Galis, Z.S., Kranzhofer, R., Fenton, J.W., 2nd, and Libby, P. (1997). Thrombin promotes activation of matrix metalloproteinase-2 produced by cultured vascular smooth muscle cells. *Arterioscler. Thromb. Vasc. Biol.* 17, 483–489.
 48. Brooks, P.C., Stromblad, S., Sanders, L.C., von Schalscha, T.L., Aimes, R.T., Stetler–Stevenson, W.G., Quigley, J.P., and Cheresch, D.A. (1996). Localization of matrix metalloproteinase MMP-2 to the surface of invasive cells by interaction with integrin alpha v beta 3. *Cell* 85, 683–693.
 49. Cernak, I. (2005). Animal models of head trauma. *NeuroRx* 2, 410–422.
 50. Long, J.B., Bentley, T.L., Wessner, K.A., Cerone, C., Sweeney, S., and Bauman, R.A. (2009). Blast overpressure in rats: recreating a battlefield injury in the laboratory. *J. Neurotrauma* 26, 827–840.
 51. Ling, G., Bandak, F., Armonda, R., Grant, G., and Ecklund, J. (2009). Explosive blast neurotrauma. *J. Neurotrauma* 26, 815–825.
 52. Bauman, R.A., Ling, G., Tong, L., Januszkiewicz, A., Agoston, D., Delanerolle, N., Kim, Y., Ritzel, D., Bell, R., Ecklund, J., Armonda, R., Bandak, F., and Parks, S. (2009). An introductory characterization of a combat-casualty-care relevant swine model of closed head injury resulting from exposure to explosive blast. *J. Neurotrauma* 26, 841–860.
 53. van Hinsbergh, V.W. (2012). Endothelium—role in regulation of coagulation and inflammation. *Semin. Immunopathol.* 34, 93–106.

Address correspondence to:
Stanislav I. Svetlov, MD
Banyan Laboratories, Inc.
12085 Research Drive
Alachua, FL 32615

E-mail: ssvetlov@banyanbio.com

or

Victor Prima, PhD
University of Florida
Gainesville, FL 32610

E-mail: vprima@ufl.edu